Atmospheric and oceanic excitation of the Earth's wobbles during 1980–2000

Richard S. Gross, Ichiro Fukumori, and Dimitris Menemenlis

Jet Propulsion Laboratory, California Institute of Technology, Pasadena, California, USA

[1] Because of the action of various geophysical excitation mechanisms, the Earth does not rotate about its figure axis, so it wobbles as it rotates. Here, the effectiveness of atmospheric and oceanic processes in exciting the Earth's wobbles during 1980–2000 is evaluated using estimates of atmospheric angular momentum from the National Centers for Environmental Prediction/National Center for Atmospheric Research (NCEP/NCAR) reanalysis project and estimates of oceanic angular momentum from the Estimating the Circulation and Climate of the Ocean (ECCO) consortium's simulation of the general circulation of the oceans. On intraseasonal timescales, atmospheric surface pressure changes are found to be the single most effective process exciting the Earth's wobbles, explaining about twice as much of the observed variance as do either atmospheric wind or ocean bottom pressure changes and nearly 4 times as much of the observed variance as do oceanic currents. However, on interannual timescales, ocean bottom pressure changes are found to be the single most effective process exciting the Earth's wobbles, explaining more than 5 times as much of the observed variance as do atmospheric wind and pressure changes combined, and more than twice as much of the observed variance as do oceanic currents. Within the Chandler band it is found that during 1980–2000 atmospheric and oceanic processes have enough power to excite the Chandler wobble and are significantly coherent with it. The single most important mechanism exciting the Chandler wobble is found to be ocean bottom pressure variations. Atmospheric and oceanic processes do not appear to have enough power to excite the Earth's wobbles to their observed levels on pentadal and longer timescales, although series longer than the 21-yearlong series used here need to be studied in order to obtain greater statistical significance of this result. *INDEX TERMS:* 1223 Geodesy and Gravity: Ocean/Earth/atmosphere interactions (3339); 1239 Geodesy and Gravity: Rotational variations; 3319 Meteorology and Atmospheric Dynamics: General circulation; 4532 Oceanography: Physical: General circulation; *KEYWORDS:* Earth rotation, polar motion, atmospheric angular momentum, oceanic angular momentum, Chandler wobble

1. Introduction

[2] In the absence of external torques and internal excitation processes, the solid Earth would uniformly rotate about its figure axis. External torques due to the gravitational attraction of the Sun, Moon, and planets cause the solid body of the Earth to tidally deform, giving rise to changes in the rotation rate of the Earth. Because the Earth's figure axis is inclined with respect to both the normal of the ecliptic and the normal of the orbital plane of the Moon, these external torques also cause the Earth to precess and nutate as it rotates. Internal excitation processes such as atmospheric wind and pressure fluctuations also cause the Earth's rate of rotation to change, and cause the Earth to wobble as it rotates.

[3] The wobbling motion of the Earth was first detected more than a century ago and since that time the Earth has been observed to wobble on all observable timescales, from subdaily to decadal. Like a system of damped harmonic oscillators, the Earth has a few discrete frequencies at which it would naturally wobble in the absence of forcing. These natural, or free, wobbles of the Earth are known as the Chandler wobble, the free core nutation, also known as the nearly diurnal free wobble, and the inner core wobble [e.g., *Eubanks*, 1993; *Mathews et al.*, 2002]. In the absence of excitation, these natural wobbles of the Earth would freely decay due to the action of dissipation processes.

[4] The Earth also wobbles over a broad range of frequencies in response to a variety of forcing mechanisms. Unlike the free wobbles whose frequencies are a function of the Earth's structure, the frequencies of the forced wobbles are the same as those of the forcing mechanisms. The broadband nature of the observed wobbling motion of the

Earth, from subdaily to decadal timescales, is a result of the broadband nature of the forcing mechanisms.

[5] The effect of the atmosphere on the Earth's wobbles was one of the first excitation mechanisms to be investigated (for reviews, see, e.g., *Munk and MacDonald* [1960] and *Eubanks* [1993]). Although atmospheric wind and pressure fluctuations have an important influence on the Earth's wobbles, they are not the sole source of excitation. Ocean tides have been shown to be the dominant cause of the Earth's wobbles on subdaily timescales [e.g., *Sovers et al.*, 1993; *Herring and Dong*, 1994; *Chao et al.*, 1996; *Gipson*, 1996] and their effect on the Earth's wobbles at termensual, fortnightly, and monthly periods has also been detected [*Gross et al.*, 1996, 1997]. On the other hand, earthquakes have been shown to have only a minor influence on the Earth's wobbles [*Chao and Gross*, 1987].

[6] Recently, near-global general circulation models of the oceans have been used to investigate the contribution of nontidal oceanic effects to exciting both the forced wobbles of the Earth [*Ponte et al.*, 1998, 2001; *Johnson et al.*, 1999; *Ponte and Stammer*, 1999; *Nastula et al.*, 2000] and the free Chandler wobble [*Ponte and Stammer*, 1999; *Gross*, 2000; *Brzezinski and Nastula*, 2002; *Brzezinski et al.*, 2002]. The studies of the forced wobbles, using time series that are 10–12 years long, have shown that adding nontidal oceanic excitation to that of the atmosphere improves the agreement with that observed. The studies of the Chandler wobble have shown the importance of oceanic processes, particularly ocean bottom pressure fluctuations, to exciting the Chandler wobble. Here, 21-yearlong results, spanning 1980 through 2000, from a near-global oceanic general circulation model are used to study atmospheric and oceanic excitation of the Earth's wobbles, including the Chandler wobble. The longer period of analysis allows better frequency resolution than was possible in previous studies. Furthermore, the source of polar motion is diagnosed by decomposing its excitation into those caused by changes in winds, currents, and pressure loading by the atmosphere and oceans, which are separately evaluated.

2. Polar Motion Excitation

[7] The Earth wobbles as it rotates as a consequence of the torques acting on it and in response to changes in its mass distribution, which change its inertia tensor. Observations of the wobbling motion of the Earth can be interpreted using the principle of conservation of angular momentum which, in a rotating, body-fixed reference frame, is expressed by

$$\frac{\partial \mathbf{L}}{\partial t} + \boldsymbol{\omega} \times \mathbf{L} = \boldsymbol{\tau} \qquad (1)$$

where $\boldsymbol{\omega}$ is the Earth's rotation vector, $\mathbf{L}$ is its angular momentum vector, and $\boldsymbol{\tau}$ are the torques acting on the Earth. In general, the angular momentum vector can be written as a sum of two terms:

$$\mathbf{L} = \mathbf{I} \cdot \boldsymbol{\omega} + \mathbf{h} \qquad (2)$$

where $\mathbf{I}$ is the Earth's inertia tensor and $\mathbf{h}$ is the relative angular momentum due to motion relative to the rotating reference frame.

[8] The Earth's rotation deviates only slightly from a state of uniform rotation, the deviation being about a few parts in 10^8 in speed, corresponding to changes of a few milliseconds (ms) in the length of the day, and about a part in 10^6 in the orientation of the rotation axis relative to the solid Earth's axis of figure, corresponding to a variation of several hundred milliarc seconds (mas) in polar motion. First-order perturbation theory can therefore be used to linearize the conservation of angular momentum equation. Within a rotating, body-fixed terrestrial reference frame having origin at the center of mass of the entire Earth, reference z axis aligned with the 1900–1905 mean figure axis of the Earth, and oriented such that its x axis lies in the direction of the Greenwich meridian and its y axis lies in the direction of the meridian at 90°E longitude, the linearized conservation of angular momentum equation can be written as [e.g., *Munk and MacDonald*, 1960; *Barnes et al.*, 1983]

$$\mathbf{m}(t) + \frac{i}{\sigma_o} \frac{d\mathbf{m}(t)}{dt} = \boldsymbol{\chi}(t) - \frac{i}{\Omega} \frac{d\boldsymbol{\chi}(t)}{dt} \qquad (3)$$

where $\sigma_o \equiv 2\pi/T_o(1 + i/2Q_o)$ is the complex-valued frequency of the Chandler wobble having period T_o and resonance quality factor Q_o, the mean angular velocity of the Earth is Ω, and $\mathbf{m}(t) \equiv m_x(t) + i\,m_y(t)$, where $m_x(t)$ and $m_y(t)$ are the direction cosines of the Earth's rotation axis relative to the axes of the rotating, body-fixed reference frame:

$$\boldsymbol{\omega}(t) = \Omega\big[m_x(t), m_y(t), 1 + m_z(t)\big]^{\mathrm{T}} \qquad (4)$$

In the absence of external torques, the $\boldsymbol{\chi}(t)$, known as the polar motion excitation functions, are functions of changes in relative angular momentum and of changes in the Earth's inertia tensor [*Wahr*, 1982]:

$$\boldsymbol{\chi}(t) = \frac{1.61}{\Omega(C - A)} \left[\mathbf{h}(t) + \frac{\Omega\,\mathbf{c}(t)}{1.44} \right] \qquad (5)$$

where $\mathbf{h}(t) \equiv h_x(t) + i\,h_y(t)$ with $h_x(t)$ and $h_y(t)$ being the x and y components, respectively, of the relative angular momentum, $\mathbf{c}(t) \equiv \Delta I_{xz}(t) + i\,\Delta I_{yz}(t)$ with $\Delta I_{xz}(t)$ and $\Delta I_{yz}(t)$ being changes in the two indicated elements of the Earth's inertia tensor, $C - A$ is the difference between the polar and equatorial moments of inertia of the entire Earth, the factor of 1.44 accounts for the yielding of the solid Earth to imposed surface loads, and the factor of 1.61 includes the effect of core decoupling.

[9] Equations (3) and (5) relate changes in angular momentum to changes in the location of the Earth's rotation pole. However, observations of the Earth's rotation, as reported by Earth rotation services, do not give the location of the Earth's rotation pole but rather give the location of the celestial ephemeris pole within the rotating, body-fixed terrestrial reference frame [*Brzezinski*, 1992; *Gross*, 1992]. Writing equation (3) in terms of the reported polar motion parameters yields

$$\mathbf{p}(t) + \frac{i}{\sigma_o} \frac{d\mathbf{p}(t)}{dt} = \boldsymbol{\chi}(t) \qquad (6)$$

where $\mathbf{p}(t) \equiv p_x(t) - i\,p_y(t)$ with $p_x(t)$ and $p_y(t)$ being the x and y components, respectively, of the reported location of

the celestial ephemeris pole within the terrestrial reference frame with, by convention, $p_y(t)$ being positive toward 90°W longitude.

[10] Equation (6), which is called here the polar motion equation, will be used to compare observed polar motion excitation with models of it computed using the products of atmospheric and oceanic general circulation models. Observed polar motion excitation functions will be computed from polar motion observations $\mathbf{p}(t)$ using equation (6). Modeled polar motion excitation functions will be computed from modeled changes in the angular momentum of atmospheric winds and pressure and oceanic currents and bottom pressure using equation (5). The relative importance of these processes in exciting polar motion will be assessed by comparing the modeled with the observed polar motion excitation functions in both the time and frequency domains. Throughout this paper, statements about the relative effectiveness of one of these processes in exciting polar motion are based on the angular momentum associated with that process, not on the torques by which the angular momentum is transferred to the solid Earth. In particular, statements about the effectiveness of atmospheric and ocean bottom pressure variations in exciting polar motion are based upon the angular momentum due to mass redistribution within the atmosphere and oceans, which manifests itself as changes in surface and bottom pressure, respectively, and not upon the torque exerted on the solid Earth by differential pressure forces.

3. Data Sets

3.1. Observed Polar Motion Excitation

[11] The observed polar motion excitation functions used in this study are derived from the daily version of the COMB2000 polar motion series that has the file name "comb2000_daily.eop" [Gross, 2001a]. COMB2000 is a combination of Earth orientation measurements taken by the techniques of optical astrometry, lunar and satellite laser ranging, very long baseline interferometry, and the global positioning system. Besides estimating polar motion, the Kalman filter used to combine the measurements also estimates the time rate of change of polar motion [Gross et al., 1998]. The polar motion excitation functions have been determined from the daily COMB2000 polar motion and polar motion rate estimates using equation (6) where the period T_o of the Chandler wobble was assumed to be 433.0 days and its quality factor Q_o was assumed to be 179 [Wilson and Vicente, 1990]. The resulting daily COMB2000 polar motion excitation series spans 20 January 1962 to 6 January 2001 at daily intervals.

[12] Known sources of polar motion excitation that can be accurately modeled should be removed from the observations before they are used to investigate atmospheric and oceanic excitation. Ocean tides are known to excite polar motion [e.g., Gross, 1993; Sovers et al., 1993; Herring and Dong, 1994; Chao et al., 1996; Gipson, 1996; Gross et al., 1996, 1997] and their effect in the diurnal and semidiurnal tidal bands are routinely modeled and removed as a standard part of the data reduction procedures employed by the various analysis centers when recovering polar motion from the raw observables [McCarthy, 1996]. However, the effect of ocean tides in the long-period tidal band are not currently modeled and removed by the analysis centers when recov-

ering polar motion and their effect is therefore included in the polar motion series that were combined to form the daily version of COMB2000. Here, the effect of the termensual (9.12- and 9.13-day), fortnightly (13.63- and 13.66-day), and monthly (27.55-day) ocean tides have been removed from the daily COMB2000 polar motion excitation series using the empirical model of Gross et al. [1997].

3.2. Atmospheric Angular Momentum

[13] The atmospheric angular momentum (AAM) series used in this study is that derived from the National Centers for Environmental Prediction/National Center for Atmospheric Research (NCEP/NCAR) reanalysis project [Kalnay et al., 1996] and was obtained from the International Earth Rotation Service (IERS) Special Bureau for the Atmosphere (SBA) [Salstein et al., 1993]. Both the angular momentum carried by the winds, computed by integrating the horizontal winds from the surface to the top of the model at 10 hPa [Salstein and Rosen, 1997], and the angular momentum due to surface pressure variations, computed by assuming that the oceans respond as an inverted barometer to the imposed surface pressure variations, were used here. The NCEP/NCAR reanalysis AAM series available from the IERS SBA spans 1 January 1948 to the present at 6-hour intervals. In order to match the temporal resolution of the observed daily COMB2000 polar motion excitation functions, daily averages of the AAM were formed by summing five consecutive values using weights of 1/8, 1/4, 1/4, 1/4, 1/8.

3.3. Oceanic Angular Momentum

[14] The oceanic angular momentum (OAM) series used in this study was computed from the products of an ocean model integrated at JPL as part of their participation in the Estimating the Circulation and Climate of the Ocean (ECCO) consortium. This ocean model, based on the Massachusetts Institute of Technology (MIT) ocean general circulation model [Marshall et al., 1997a, 1997b], has realistic boundaries and bottom topography, has 46 levels ranging in thickness from 10 m at the surface to 400 m at depth, and spans 73.5°S to 73.5°N latitude with no normal flow at horizontal boundaries and with a latitudinal grid spacing ranging between 1/3° at the equator to 1° at the poles and a longitudinal grid spacing of 1°. The model is initialized with climatological temperature and salinity distributions [Levitus and Boyer, 1994; Levitus et al., 1994] and is spun-up from rest for 10 years using climatological forcing fields from the Comprehensive Ocean-Atmosphere Data Set (COADS; http://www.cdc.noaa.gov/coads). Subsequently, the model is forced with twice daily wind stress and daily surface heat flux and evaporation-precipitation fields from the NCEP/NCAR reanalysis project during 1980–2000. The 1980–1997 time mean of the respective individual NCEP/NCAR reanalysis forcing fields are replaced by the corresponding means of COADS in favor of the latter's resolution of the climatological means. Sea surface temperature is further relaxed to observed weekly satellite measurements [Reynolds and Smith, 1994] using a time- and space-varying relaxation coefficient [Barnier et al., 1995]. Sea surface salinity is relaxed to monthly climatological values [Levitus et al., 1994] using a 60-day relaxation coefficient. Surface atmospheric pressure was not used to force the model.
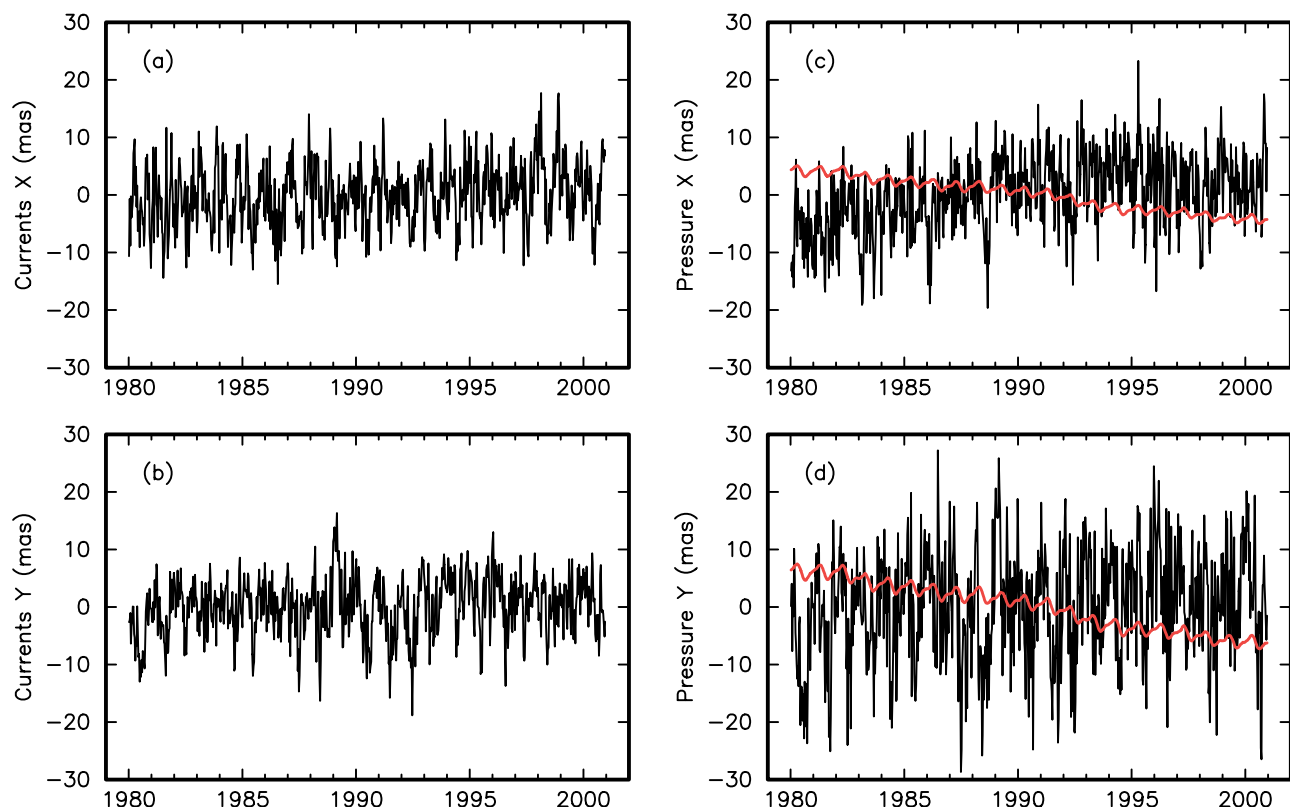
Figure 1. The x and y components of the oceanic excitation functions due to variations in (a and b) oceanic currents and (c and d) ocean bottom pressure. For purposes of clarity of display, 10-day averages of the daily oceanic excitation functions are shown. In Figures 1c and 1d, the red curves show the correction that was applied to the pressure term as a result of enforcing mass conservation. The black curves show the final pressure excitation functions after the correction was applied.

[15] The MIT ocean general circulation model used here is formulated using the Boussinesq approximation [*Marshall et al.*, 1997a, 1997b], so it conserves volume rather than mass. Artificial mass variations can be introduced in Boussinesq models due to the applied surface heat and salt fluxes. For example, the changing applied heat flux will change the density, which, since volume is conserved, will artificially change the mass of the modeled oceans. Here, mass conservation has been enforced by adding a uniform layer having the appropriate time-dependent thickness to the ocean surface [*Greatbatch*, 1994; *Greatbatch et al.*, 2001].

[16] The angular momentum carried by oceanic currents was computed by integrating the eastward zonal $u(\mathbf{r},t)$ and northward meridional $v(\mathbf{r},t)$ currents throughout the volume V_o of the modeled oceans:

$$\mathbf{L_c}(t) = - \int_{V_o} \rho(\mathbf{r},t) r [\sin\phi\, u(\mathbf{r},t) + i\, v(\mathbf{r},t)] e^{i\lambda} dV \qquad (7)$$

where $\mathbf{L_c}(t) \equiv L_{c,x}(t) + i\, L_{c,y}(t)$ with $L_{c,x}(t)$ and $L_{c,y}(t)$ being the x and y components, respectively, of the angular momentum due to currents, ϕ is north latitude, λ is east longitude, and $\rho(\mathbf{r},t)$ is the density of some mass element located at position $\mathbf{r}$. The angular momentum due to changes in the mass distribution of the oceans, or,

equivalently, due to changes in ocean bottom pressure, was computed by integrating the time-dependent density field throughout the volume of the modeled oceans:

$$\mathbf{L_p}(t) = -\Omega \int_{V_o} \rho(\mathbf{r},t) r^2 \sin\phi\cos\phi\, e^{i\lambda}\, dV \qquad (8)$$

where $\mathbf{L_p}(t) \equiv L_{p,x}(t) + i\, L_{p,y}(t)$ with $L_{p,x}(t)$ and $L_{p,y}(t)$ being the x and y components, respectively, of the angular momentum due to mass redistribution. When using equations (7) and (8) to calculate the OAM, the effects of enforcing mass conservation and of changes in sea surface height were both included.

[17] The modeled oceanic angular momentum values were converted to polar motion excitation functions using equation (5) with $\mathbf{h}(t) \equiv \mathbf{L_c}(t)$, $\Omega\mathbf{c}(t) \equiv \mathbf{L_p}(t)$, and values of 7.292115×10^{-5} rad/s and 2.61×10^{35} kg m^2 for Ω and $C - A$, respectively. The resulting modeled oceanic excitation functions span 1980–2000 at hourly intervals. In order to match the temporal resolution of the observed excitation functions, daily averages of the hourly oceanic excitation functions were computed by summing 25 consecutive values using weights of 1/48, 1/24, 1/24, . . . 1/24, 1/24, 1/48.

[18] The resulting modeled oceanic excitation functions are shown in Figure 1. For display purposes only, 10-day
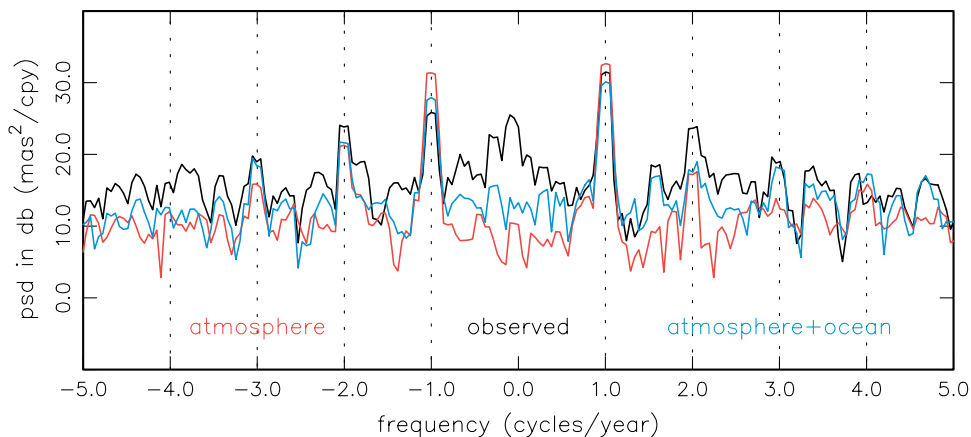
POLAR MOTION EXCITATION

Figure 2. Power spectral density (PSD) estimates in decibels (dB) computed by the multitaper method from time series of polar motion excitation functions $\chi(t)$ spanning 1980.0–2001.0 of (1) the observed daily COMB2000 polar motion excitation function derived from astrometric and space-geodetic Earth orientation measurements (black curve), (2) the sum of the excitation functions due to atmospheric wind and surface pressure changes (red curve) where the atmospheric pressure term is computed assuming that the inverted barometer approximation is valid, and (3) the sum of the excitation functions due to atmospheric wind and surface pressure (inverted barometer) changes as well as oceanic current and bottom pressure changes (blue curve). The retrograde component of polar motion excitation is represented by negative frequencies, the prograde component by positive frequencies.

averages of the daily oceanic excitation functions are shown in black. As can be seen, the excitation functions due to changes in ocean bottom pressure (Figures 1c and 1d) exhibit greater variability than those due to changes in oceanic currents (Figures 1a and 1b), especially in the y component.

[19] The red curves shown in Figures 1c and 1d show the correction that was applied to the pressure term as a result of enforcing mass conservation on the ocean model. Besides a linear trend, which is probably a result of incomplete adjustment of the ocean model to the climatological forcing fields during spin-up, the correction for mass conservation consists primarily of a seasonal adjustment, probably reflecting the dominant seasonal character of the applied heat flux forcing.

4. Annual Wobble and Its Higher Harmonics

[20] The annual wobble is a forced wobble of the Earth that is caused largely by the annual appearance of a high atmospheric pressure system over Siberia every winter, although other sources of excitation including winds have been shown to be important (for reviews, see, e.g., *Munk and MacDonald* [1960] and *Eubanks* [1993]). Atmospheric wind and pressure variations have also been shown to be important mechanisms exciting the semiannual wobble [*Chao and Au*, 1991], although, since the agreement is again not perfect, other mechanisms must also be contributing to its excitation. In this section, the contribution of oceanic processes to exciting the annual wobble and its higher harmonics during 1980–2000 is compared to that of atmospheric processes.

[21] Power spectra of the observed (black), atmospheric (red), and sum of atmospheric and oceanic (blue) excitation

functions are shown in Figure 2. The spectrum of the atmospheric excitation function includes the contributions of both wind and surface pressure variations where the response of the oceans to the surface pressure changes is assumed to be that of an inverted barometer. The oceanic excitation function includes the contributions of both currents and ocean bottom pressure variations. The spectra have been computed by the multitaper method using a resolution bandwidth of twice the fundamental frequency of 1/21 cycles per year (cpy) and by forming a simple unweighted average of the resulting first 3 eigenspectra [*Percival and Walden*, 1993]. Only the low-frequency portion of the spectra is shown in Figure 2.

[22] As shown in Figure 2, better agreement with the observed power at frequencies less than 5 cpy is obtained when the effects of oceanic current and bottom pressure variations is added to that of atmospheric wind and surface pressure changes, although discrepancies still remain, especially for the lowest frequencies near 0 cpy (a mean and trend have been removed from each series prior to computing its spectrum). This discrepancy at decadal periods will be discussed in the section on the pentadal and Markowitz wobbles below. Here the agreement between the observed and modeled excitation functions at the annual frequency and its higher harmonics is discussed.

[23] Peaks in the observed power spectrum (black curve) are clearly seen in Figure 2 at the annual (1 cpy), semiannual (2 cpy) and terannual (3 cpy) frequencies, with little evidence of spectral peaks being seen at higher harmonics of the annual. In order to compare the observed and modeled excitation at the annual, semiannual, and terannual frequencies, a mean, trend, and periodic terms at these frequencies were fit to the observed and modeled excitation functions. Since no uncertainty estimates are available for

Table 1. Annual Wobble Excitation[a]

	Prograde		Retrograde	
Excitation Process	Amplitude, mas	Phase, deg	Amplitude, mas	Phase, deg
Observed	14.52 ± 0.33	-62.77 ± 1.30	7.53 ± 0.33	-120.09 ± 2.50
Atmospheric				
Wind	2.97 ± 0.12	-34.92 ± 2.30	2.04 ± 0.12	12.06 ± 3.36
Surface pressure (IB)	15.12 ± 0.17	-101.92 ± 0.66	15.05 ± 0.17	-105.30 ± 0.66
Wind plus surface pressure (IB)	16.51 ± 0.23	-92.38 ± 0.81	14.23 ± 0.23	-98.00 ± 0.94
Oceanic				
Currents	2.31 ± 0.09	39.72 ± 2.13	2.11 ± 0.09	50.70 ± 2.33
Bottom pressure	3.45 ± 0.11	63.18 ± 1.87	3.42 ± 0.11	110.24 ± 1.89
Currents plus bottom pressure	5.64 ± 0.16	53.81 ± 1.61	4.84 ± 0.16	88.22 ± 1.87
Atmospheric plus oceanic				
Wind plus currents	4.22 ± 0.15	-3.09 ± 2.08	3.91 ± 0.15	31.71 ± 2.24
Surface (IB) plus bottom pressure	11.82 ± 0.20	-97.61 ± 0.99	12.43 ± 0.20	-114.51 ± 0.94
Total of all atmospheric plus oceanic	12.23 ± 0.28	-77.50 ± 1.32	9.43 ± 0.28	-101.18 ± 1.71

[a]IB is inverted barometer; reference date for phase is 1 January 1990, 0000 UT.

the atmospheric and oceanic excitation functions, this fit was obtained using unweighted least squares. For consistency, unweighted least squares was also used to obtain the fit to the observed excitation function even though uncertainty estimates are available for the observed values. The uncertainties assigned to the fitted parameters and given in Tables 1–3 are the 1σ formal uncertainties computed using the standard deviation of the postfit residuals as an estimate of the mean uncertainty of the observed or modeled excitation values. The uncertainties thus determined can be considered realistic in the sense that the resulting postfit residuals have a reduced chi-square of one.

[24] Table 1 shows the results of this fit for the amplitude A and phase α of the prograde (subscript p) and retrograde (subscript r) components of the excitation of the annual wobble defined by

$$\chi(t) = A_p\, e^{i\alpha_p}\, e^{i\sigma(t-t_o)} + A_r\, e^{i\alpha_r}\, e^{-i\sigma(t-t_o)} \qquad (9)$$

where σ is the annual frequency and the reference date t_o is 1 January 1990, 0000 UT. For simplicity, the individual contributions to the excitation functions by atmospheric winds and atmospheric surface pressure assuming an inverted barometer response over the oceans will be referred to hereinafter as that due to "winds" and "surface pres-

sure", respectively. Likewise, contributions by oceanic currents and ocean bottom pressure are simply referred to as due to "currents" and "bottom pressure", respectively. For both the prograde and retrograde components, surface pressure variations are seen to be the single most important excitation mechanism, being more than 4 times as large as the effect of bottom pressure variations, and 5–7 times as large as the effect of either winds or currents. The effects of winds and currents on exciting the annual wobble are comparable, having nearly the same retrograde amplitude and a prograde amplitude that differs by about 30%. The effect of currents on exciting the annual wobble is about 2/3 of the effect of bottom pressure variations. Figure 3 shows a phasor diagram of the retrograde (top) and prograde (bottom) components of the observed (obs), atmospheric (atm; the sum of the wind and surface pressure terms), and oceanic (ocn; the sum of the current and bottom pressure terms) excitation functions at the annual frequency. Adding oceanic excitation to that of the atmosphere is seen to bring the modeled excitation closer to that observed although discrepancies of 4.11 mas in amplitude and −13.59 degrees (deg) in phase for the prograde component and 3.36 mas in amplitude and 125.39 deg in phase for the retrograde component still remain. Here and in the following paragraphs on the semiannual and terannual wobbles, the

Table 2. Semiannual Wobble Excitation[a]

	Prograde		Retrograde	
Excitation Process	Amplitude, mas	Phase, deg	Amplitude, mas	Phase, deg
Observed	5.67 ± 0.33	107.56 ± 3.32	5.80 ± 0.33	123.66 ± 3.24
Atmospheric				
Wind	0.36 ± 0.12	71.76 ± 19.00	0.55 ± 0.12	-134.43 ± 12.39
Surface pressure (IB)	2.60 ± 0.17	47.45 ± 3.81	4.75 ± 0.17	103.77 ± 2.08
Wind plus surface pressure (IB)	2.93 ± 0.23	50.36 ± 4.58	4.49 ± 0.23	109.77 ± 2.99
Oceanic				
Currents	1.32 ± 0.09	176.16 ± 3.71	1.41 ± 0.09	-143.46 ± 3.49
Bottom pressure	0.77 ± 0.11	133.89 ± 8.41	1.48 ± 0.11	-136.46 ± 4.35
Currents plus bottom pressure	1.96 ± 0.16	160.89 ± 4.62	2.89 ± 0.16	-139.87 ± 3.14
Atmospheric plus oceanic				
Wind plus currents	1.28 ± 0.15	160.38 ± 6.83	1.96 ± 0.15	-140.92 ± 4.48
Surface (IB) plus bottom pressure	2.75 ± 0.20	63.61 ± 4.26	4.22 ± 0.20	121.55 ± 2.78
Total of all atmospheric plus oceanic	2.90 ± 0.28	89.70 ± 5.57	4.41 ± 0.28	147.63 ± 3.66

[a]IB is inverted barometer; reference date for phase is 1 January 1990, 0000 UT.

Table 3. Terannual Wobble Excitation[a]

	Prograde		Retrograde	
Excitation Process	Amplitude, mas	Phase, deg	Amplitude, mas	Phase, deg
Observed	2.22 ± 0.33	108.79 ± 8.49	3.64 ± 0.33	−42.18 ± 5.17
Atmospheric				
Wind	0.14 ± 0.12	124.58 ± 47.26	0.77 ± 0.12	−9.18 ± 8.88
Surface pressure (IB)	1.29 ± 0.17	144.03 ± 7.66	1.65 ± 0.17	2.56 ± 6.02
Wind plus surface pressure (IB)	1.43 ± 0.23	142.10 ± 9.38	2.41 ± 0.23	−1.17 ± 5.58
Oceanic				
Currents	0.81 ± 0.09	145.84 ± 6.09	0.44 ± 0.09	−97.00 ± 11.29
Bottom pressure	0.71 ± 0.11	120.18 ± 9.13	1.39 ± 0.11	−69.15 ± 4.66
Currents plus bottom pressure	1.48 ± 0.16	133.87 ± 6.13	1.78 ± 0.16	−75.69 ± 5.08
Atmospheric plus oceanic				
Wind plus currents	0.94 ± 0.15	142.65 ± 9.28	0.90 ± 0.15	−38.09 ± 9.74
Surface (IB) plus bottom pressure	1.96 ± 0.20	135.64 ± 5.98	2.46 ± 0.20	−29.74 ± 4.76
Total of all atmospheric plus oceanic	2.90 ± 0.28	137.91 ± 5.57	3.36 ± 0.28	−31.97 ± 4.81

[a]IB is inverted barometer; reference date for phase is 1 January 1990, 0000 UT.

discrepancy amplitudes and phases given are those of the residual phasors formed by removing the sum total of all modeled atmospheric and oceanic excitation from that observed at the prograde and, separately, retrograde frequencies. The results obtained here for the prograde component of the observed, atmospheric, and oceanic excitation of the annual wobble during the interval 1980–2000 are similar to those obtained by *Ponte and Stammer* [1999] for the interval 1985–1995.

[25] Table 2 shows the corresponding results for the excitation of the semiannual wobble. As for the excitation of the annual wobble, surface pressure variations are the single most important excitation mechanism of the semiannual wobble, being more than 3 times as large as the effect of bottom pressure variations, 2–3 times as large as the effect of currents, and 8 times as large as the effect of winds. Currents and bottom pressure variations contribute about equally to exciting the retrograde component of the semiannual wobble, having nearly the same retrograde amplitude and phase. The effect of currents on the excitation of the prograde component of the semiannual wobble is about 70% larger than that of bottom pressure variations, and more than 3 times as large as the effect of winds, although with different phases. Figure 4 shows a phasor diagram of the retrograde and prograde components of the observed, atmospheric, and oceanic excitation functions at the semiannual frequency. Adding oceanic excitation to that of the atmosphere is seen to bring the prograde component of the modeled excitation closer to that observed, but not the retrograde component. Discrepancies of 3.05 mas in amplitude and 124.57 deg in phase for the prograde component and 2.52 mas in amplitude and 78.23 deg in phase for the retrograde component still remain.

[26] Table 3 shows the results for the excitation of the terannual wobble. Again, surface pressure variations are the most effective excitation mechanism of the terannual wobble, although other sources of atmospheric and oceanic excitation are nearly as large. The effects of surface pressure and bottom pressure on exciting the terannual wobble are similar, differing by less than 20% for the retrograde component and by about 50% for the prograde. For the prograde component, the effect of currents is about 10% larger than that of bottom pressure variations and about 6 times larger than that of winds, whereas for the retrograde

component it is only about 1/3 as large as the effect of bottom pressure variations and about 2/3 as large as that of winds. Figure 5 shows the phasor diagram for the retrograde and prograde components of the observed, atmospheric, and oceanic excitation of the terannual wobble. Adding oceanic excitation to that of the atmosphere is seen to bring the retrograde component of the modeled excitation closer to that observed, but not the prograde component. Discrepancies of 1.45 mas in amplitude and 6.20 deg in phase for the prograde component and 0.69 mas in amplitude and −102.79 deg in phase for the retrograde component still remain.

[27] The rather large discrepancies that remain at the annual, semiannual, and terannual frequencies after atmospheric and oceanic excitation is removed from that observed may reflect errors in the observed and/or modeled excitation at these frequencies, but may also indicate that other processes are important in exciting the annual wobble and its higher harmonics. *Wünsch* [2002] has recently summarized the contribution of soil moisture and snow load to exciting the annual and semiannual wobbles. Although the available soil moisture models exhibit large differences, *Wünsch* [2002] concludes that soil moisture and snow load effects are important contributors to exciting the annual and semiannual wobbles [also see *Chen et al.*, 2000b].

[28] Loading effects appear to be the most important mechanisms exciting the annual, semiannual, and terannual wobbles, with atmospheric surface pressure variations being the single most important mechanism. From Tables 1–3 it is seen that the sum of atmospheric surface and ocean bottom pressure effects are 2–3 times larger than the sum of the effects of atmospheric winds and oceanic currents. As summarized by *Wünsch* [2002], soil moisture and snow load are additional loading effects that are important in exciting the annual and semiannual wobbles. Since the Challenging Minisatellite Payload (CHAMP) and Gravity Recovery And Climate Experiment (GRACE) satellite missions will be measuring changes in the Earth's gravitational field caused by the mass displacements giving rise to these loading effects, and since changes in the second-degree coefficients of the Earth's gravitational field are related to changes in the Earth orientation excitation functions caused by mass displacements [*Chen et al.*, 2000a; *Gross*, 2001b, 2003],
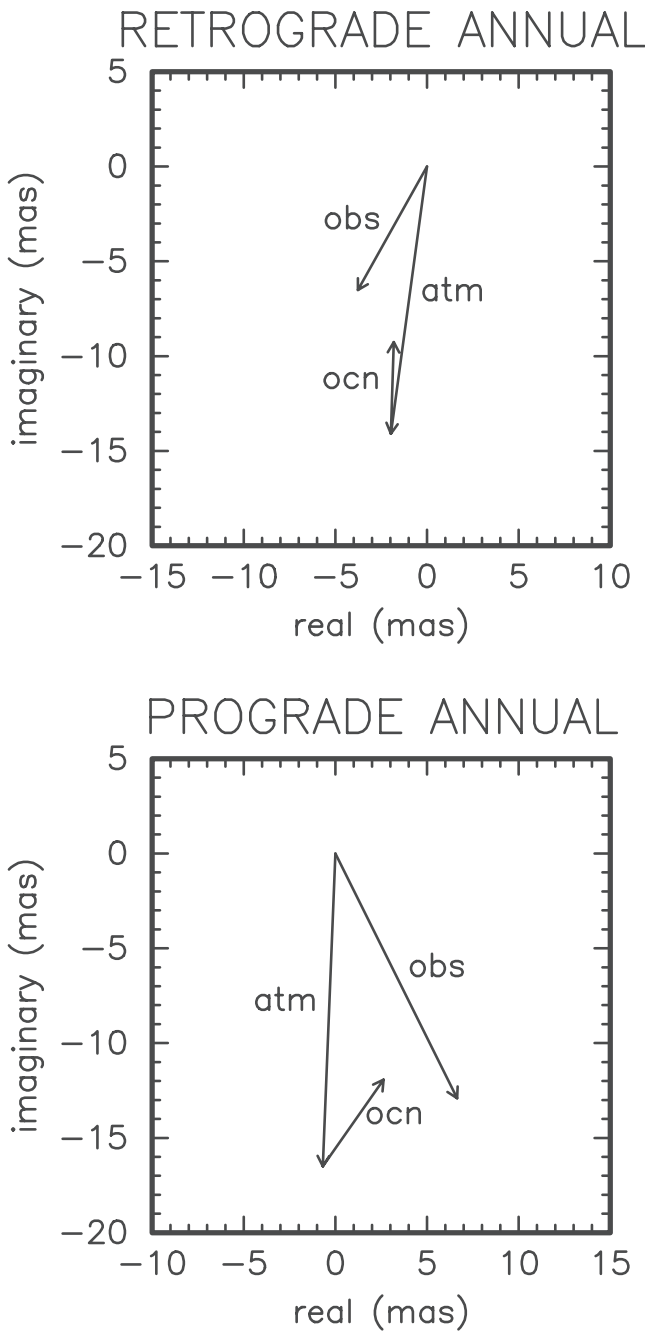
RETROGRADE ANNUAL

these direct measurements by CHAMP and GRACE of the excitation of the Earth's wobbles due to mass redistribution.

5. Chandler Wobble

[29] The Chandler wobble is a resonance in the Earth's rotation having a period T_o of 433.0 days and a quality factor Q_o of 179 [*Wilson and Vicente*, 1990] that exists because the Earth is not rotating about its figure axis (for reviews, see, e.g., *Munk and MacDonald* [1960] and *Eubanks* [1993]). In the absence of excitation, the Chandler wobble would freely decay with a time constant of about 68 years to the minimum rotational energy state of rotation about the figure axis. Since the Chandler wobble has been under observation for more than a century, and since its
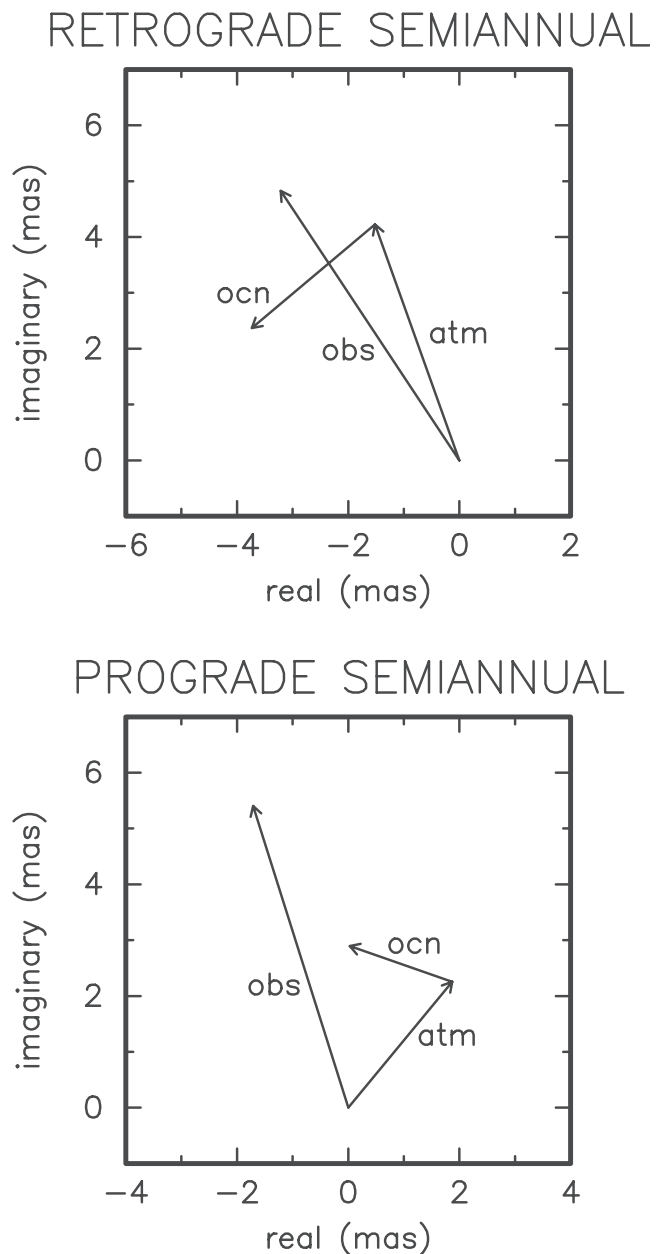
RETROGRADE SEMIANNUAL

PROGRADE ANNUAL

Figure 3. Phasor diagrams of the retrograde and prograde components of the observed (obs), atmospheric (atm), and oceanic (ocn) excitation functions at the annual frequency. The atmospheric results include the effects of both winds and surface pressure where the pressure term was computed assuming that the oceans respond as an inverted barometer to the imposed surface pressure variations; the oceanic results include the effects of both currents and ocean bottom pressure. The reference date for the phase is 1 January 1990, 0000 UT.

PROGRADE SEMIANNUAL

CHAMP and GRACE will, in effect, be directly measuring the excitation of the Earth's wobbles due to mass redistribution. Greater understanding of the excitation of the annual wobble and its higher harmonics will be gained by studying

Figure 4. As in Figure 3 but for the excitation of the semiannual wobble.

RETROGRADE TERANNUAL

PROGRADE TERANNUAL

Figure 5. As in Figure 3 but for the excitation of the terannual wobble.

Chandler wobble, with ocean bottom pressure variations being the single most effective excitation mechanism during this 11-yearlong time interval. Here, atmospheric and oceanic excitation of the Chandler wobble is investigated using the 21-yearlong NCEP/NCAR reanalysis AAM and JPL ECCO OAM series spanning 1980–2000.

[31] Table 4 shows the power in the Chandler band for the observed, atmospheric, and oceanic excitation series. The Chandler band is taken here to range between 0.81 cpy and 0.91 cpy which is narrower than the 0.730–0.913 cpy band used by *Gross* [2000]. The better frequency resolution attained with the 21-yearlong excitation series used here allows better resolution of the Chandler band than was possible with the 11-yearlong series used by *Gross* [2000]. Prior to estimating the power, a seasonal signal was first removed from all series by least squares fitting and removing a mean, a trend, and periodic terms at the annual, semiannual, and terannual frequencies (see the section above on the annual wobble and its higher harmonics). As in the work by *Gross* [2000], the power in the Chandler band was computed by integrating the power spectral density (PSD) across the Chandler band where the PSD was computed after first applying a Hanning window [e.g., *Priestley*, 1981] to each excitation series.

[32] From Table 4 it can be seen that during 1980–2000 ocean bottom pressure variations are the single most effective mechanism exciting the Chandler wobble, having about 50% more power than atmospheric surface pressure variations. The power of oceanic currents in the Chandler band is only 1/8 as large as the power of ocean bottom pressure variations, and the power of atmospheric winds is only about 1/2 as large as the power of atmospheric surface pressure variations. The combined effect of atmospheric winds and surface pressure and oceanic currents and bottom pressure have about 20% more power in the Chandler band than that observed.

[33] Figure 6 shows the magnitude of the squared coherence and the phase spectrum between the atmospheric and observed excitation (red curve) and between the combined atmospheric and oceanic excitation and that observed (blue curve). The atmospheric excitation is the sum of the wind and surface pressure terms. The oceanic excitation is the sum of the current and bottom pressure terms. The squared coherence and phase estimates were obtained by averaging over 11 frequency intervals and the 95% and 99% confidence limits of the magnitude of the squared coherence are

amplitude has at times been observed to actually increase, some mechanism or mechanisms must be acting to excite it.

[30] Atmospheric processes were amongst the first mechanisms to be considered as candidates for exciting the Chandler wobble. However, it has generally been concluded that wind and surface pressure variations have only about 25% of the required power (see *Wahr* [1983], although for a different opinion, see *Aoyama and Naito* [2001]). Recently, the contribution of oceanic processes to exciting the Chandler wobble has been studied [*Ponte and Stammer*, 1999; *Gross*, 2000; *Brzezinski and Nastula*, 2002; *Brzezinski et al.*, 2002]. In particular, *Gross* [2000] concluded that during 1985–1995 atmospheric and oceanic processes combined have enough power to excite the

Table 4. Chandler Band Excitation Power[a]

Excitation Process	Power, mas^2
Observed	1.90
Atmospheric	
Wind	0.29
Surface pressure (IB)	0.65
Wind plus surface pressure (IB)	1.03
Oceanic	
Currents	0.12
Bottom pressure	0.96
Currents plus bottom pressure	0.66
Atmospheric plus oceanic	
Wind plus currents	0.70
Surface (IB) plus bottom pressure	2.47
Total of all atmospheric plus oceanic	2.22

[a]IB is inverted barometer; Chandler band is 0.81–0.91 cpy.

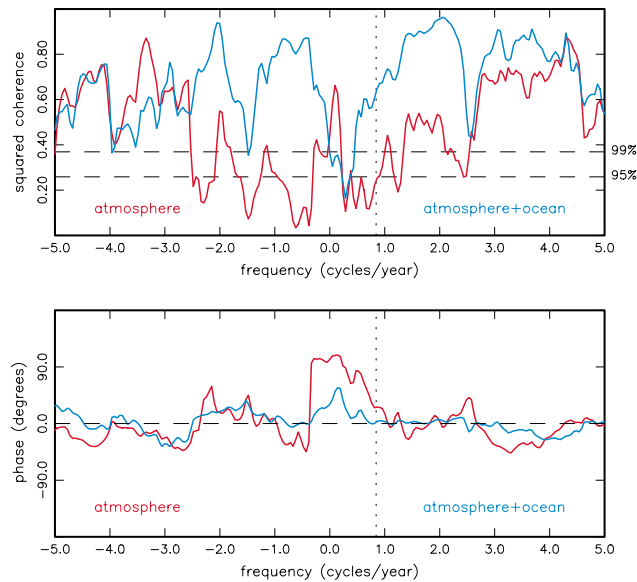COHERENCE OF MODELED WITH OBSERVED EXCITATION

Figure 6. Magnitude of (top) the squared coherence and (bottom) the phase spectrum between the observed polar motion excitation functions spanning 1980.0–2001.0 and the excitation functions due to (1) the sum of atmospheric wind and surface pressure changes (red curve) where the pressure term is that computed assuming the inverted barometer approximation for the response of the oceans, and (2) the sum of atmospheric wind and surface pressure (inverted barometer) and oceanic current and bottom pressure variations (blue curve). A seasonal signal has been removed from all series prior to coherence and phase estimation by least squares fitting and removing a mean, a trend, and periodic terms at the annual, semiannual, and terannual frequencies. The vertical dotted line indicates the Chandler frequency of 0.8435 cpy and the horizontal dashed lines in Figure 6 (top) indicate the 95% and 99% confidence levels of the magnitude of the squared coherence.

indicated by the horizontal dashed lines in the top panel. As can be seen, adding the oceanic excitation to the atmospheric significantly improves the coherence and phase with that observed, including near the Chandler frequency which is indicated by the vertical dotted line.

[34]   These results for 1980–2000 confirm those of *Gross* [2000] and *Brzezinski and Nastula* [2002] for 1985–1995 that atmospheric and oceanic processes have enough power to excite the Chandler wobble and are significantly coherent with it, and that ocean bottom pressure variations are the single most important excitation mechanism. However, 21 years is still only about 1/3 of the estimated decay time constant, 68 years, of the Chandler wobble. Thus it would be desirable to have even longer oceanic excitation series in order to further investigate the excitation of the Chandler wobble by atmospheric and oceanic processes [*Brzezinski et al.*, 2002].

6.   Interannual Wobbles

[35]   The wobbling motion of the solid Earth on interannual timescales is a forced response of the Earth to its

excitation mechanisms. *Abarca del Rio and Cazenave* [1994] compared the observed excitation of the Earth's wobbles to atmospheric excitation during 1980–1991, finding similar fluctuations in both components on timescales between 1 and 3 years, and in the y component on timescales between 1.2 and 8 years, but only when the atmospheric excitation is computed assuming the oceans fully transmit the imposed atmospheric pressure variations to the floor of the oceans (noninverted barometer approximation). *Chao and Zhou* [1999] studied the correlation of the observed polar motion excitation functions on interannual timescales during 1964–1994 with the Southern Oscillation Index (SOI) and the North Atlantic Oscillation Index (NAOI). Although little agreement was found with the SOI, significant agreement was found with the NAOI, especially for the x component of the observed excitation function, indicating a possible meteorological origin of the interannual wobbles. *Johnson et al.* [1999] compared the observed polar motion excitation functions on interannual timescales during 1988–1998 with atmospheric and oceanic excitation functions, finding only weak agreement between the observed and modeled excitation functions. Here, atmospheric and oceanic excitation of the interannual wobbles during 1980–2000 is examined.

[36]   For frequencies between −1 cpy and +1 cpy, Figure 2 shows that adding excitation due to oceanic currents and bottom pressure fluctuations to that due to atmospheric winds and surface pressure variations improves the agreement in power with that observed, although significant discrepancies remain, especially at the lowest resolvable frequencies (see section below on the pentadal and Markowitz wobbles). Figure 6 shows that the coherence between the observed and modeled excitation functions is significantly improved in the interannual frequency band when oceanic excitation is added to atmospheric, especially at retrograde interannual frequencies.

[37]   Figure 7 shows the x and y components of the observed and modeled excitation functions on interannual timescales obtained by applying a band-pass filter with cutoff frequencies of 1/6 cpy and 1 cpy. As above, seasonal signals were first removed from the excitation functions by least squares fitting and removing a mean, a trend, and periodic terms at the annual, semiannual, and terannual frequencies. The atmospheric excitation function shown in Figure 7 (red curve) is the sum of wind and surface pressure excitation. Adding oceanic current and bottom pressure excitation to that of atmospheric winds and surface pressure (blue curve) is seen to improve the agreement with that observed (black curve), especially for the y component.

[38]   Table 5 gives the percentage of the observed excitation variance explained by the modeled excitation processes along with the correlation between the observed and modeled excitation series. X gives the results for the x component, Y gives the results for the y component, and $X + iY$ gives the results for the complex-valued excitation functions formed from the x and y components. A negative percentage variance explained indicates that the variance increased when that excitation process was removed from the observed excitation. The 99% significance level for the correlations is estimated to be 0.36 after accounting for the reduction in the degrees of freedom that was determined
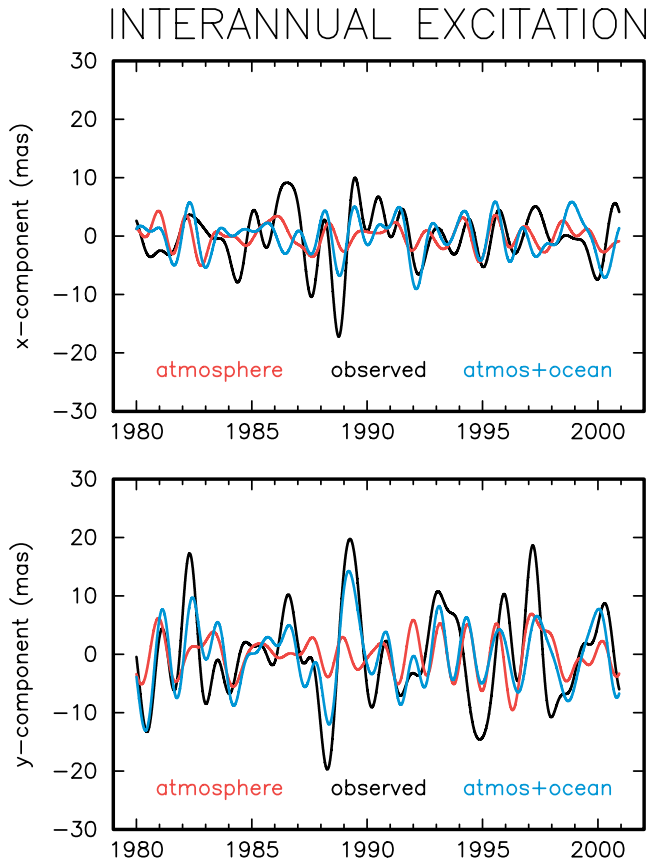
INTERANNUAL EXCITATION

Figure 7. The x and y components of the observed (black), the sum of atmospheric wind and surface pressure (red), and the sum of atmospheric wind and surface pressure and oceanic currents and bottom pressure (blue) excitation functions on interannual timescales. Interannual wobbles are defined here to be wobbles having periods between 1 year and 6 years. The atmospheric surface pressure term is that computed assuming the ocean response to the imposed surface pressure variations is as an inverted barometer.

from the width of the central peak of the autocorrelation functions.

[39] As can be seen from Table 5, atmospheric processes are not effective in exciting the wobbles of the solid Earth on interannual timescales. Atmospheric wind and/or surface pressure changes are not significantly correlated with the observed excitation and can explain at most only 12% of the observed variance, and then only for the x component. Oceanic currents are as ineffective as atmospheric processes in exciting the x component of the observed excitation, but are more effective in exciting the y component, explaining 19% of the observed excitation y component and having a correlation coefficient with it of 0.55. However, ocean bottom pressure changes are seen to be quite effective in exciting the interannual wobbles, especially the y component, explaining 12% and 36%, respectively, of the x and y components of the observed excitation, and having correlation coefficients with them of 0.37 and 0.68, respectively. The sum of all atmospheric and oceanic processes studied here can explain 7% and 51%, respectively, of the x and y components of the

observed excitation and have correlation coefficients with them of 0.40 and 0.71, respectively.

[40] As shown in Table 5, the sum of oceanic currents and bottom pressure changes are quite effective in exciting the y component of the interannual wobbles, explaining 43% of the observed variance and having a correlation coefficient with it of 0.67. Including atmospheric wind and surface pressure excitation increases the explained variance and correlation coefficient only slightly, to 51% and 0.71, respectively. However, neither atmospheric wind and/or surface pressure fluctuations nor oceanic current and/or bottom pressure changes are effective in exciting the x component of the interannual wobbles. Since a uniform sea level change would cause the polar motion excitation function to change along 52°E longitude [*Chao and O'Connor*, 1988], oceanic processes are generally considered to be more effective in exciting the y component of the Earth's wobbles, as has been found here. The finding that more than half of the observed variance of the y component remains to be explained, and that neither atmospheric nor oceanic processes are effective in exciting the x component, may indicate that a third mechanism is acting to excite the interannual wobbles.

[41] Hydrological processes acting on land could be expected to primarily excite the x component of polar motion, although it could also contribute to exciting the y component. *Kuehne and Wilson* [1991] studied the effects of terrestrial water storage on exciting polar motion during 1900–1985, finding that it may be an important excitation mechanism on interannual and longer timescales. Interannual fluctuations in glaciers [*Trupin et al.*, 1992], polar ice [*Trupin*, 1993], snow load [*Chao et al.*, 1987], and lake and

Table 5. Interannual Wobble Excitation[a]

Excitation Process	X	Y	X + i Y
Percentage of Observed Excitation Variance Explained			
Atmospheric			
Wind	12.1	−6.9	−2.2
Surface pressure (IB)	−19.6	4.1	−1.7
Wind plus surface pressure (IB)	3.5	6.5	5.8
Oceanic			
Currents	−9.5	19.4	12.2
Bottom pressure	12.5	36.2	30.3
Currents plus bottom pressure	2.9	43.3	33.3
Atmospheric plus oceanic			
Wind plus currents	−6.2	12.0	7.5
Surface (IB) plus bottom pressure	−4.6	42.3	30.7
Total of all atmospheric plus oceanic	7.5	50.8	40.1
Correlation With Observed Excitation			
Atmospheric			
Wind	0.35	0.05	0.15
Surface pressure (IB)	−0.03	0.25	0.18
Wind plus surface pressure (IB)	0.26	0.29	0.28
Oceanic			
Currents	−0.02	0.55	0.48
Bottom pressure	0.37	0.68	0.59
Currents plus bottom pressure	0.30	0.67	0.59
Atmospheric plus oceanic			
Wind plus currents	0.21	0.35	0.37
Surface (IB) plus bottom pressure	0.26	0.67	0.56
Total of all atmospheric plus oceanic	0.40	0.71	0.64

[a]X, x component; Y, y component; IB is inverted barometer; 99% significance level for correlations is 0.36; interannual frequency band ranges from 1/6 to 1 cpy.

reservoir levels [*Chao*, 1988] have been found to be ineffective in exciting the Earth's wobbles. Further progress in understanding the origin of the interannual wobbles can be expected to be made when accurate global hydrologic models become available, and, as for the annual wobble and its higher harmonics, when time-dependent gravitational field models become available from the CHAMP and GRACE satellite missions.

7. Pentadal and Markowitz Wobbles

[42] Pentadal wobbles are defined here to be wobbles whose frequencies lie between the interannual and decadal frequency bands. Figure 2 shows that within this frequency band the observed excitation power increases while both the atmospheric and sum of atmospheric and oceanic excitation power remains relatively flat, indicating that neither atmospheric nor oceanic processes have enough power to excite the pentadal wobbles to the observed level. However, the 21-yearlong series studied here are too short to arrive at a definitive conclusion regarding possible atmospheric and oceanic excitation of the pentadal wobbles. Longer excitation series must be studied before this can be done.

[43] Quasiperiodic wobbles on decadal timescales having amplitudes of about 30 mas are collectively known as the Markowitz wobble. The excitation mechanism of the Markowitz wobble is currently unknown, although *Wilson* [1993] has noted that its direction of linear polarization is close to the direction, 52°E longitude, along which the polar motion excitation function would vary in response to a uniform change in sea level, indicating that oceanic processes may be important in exciting the Markowitz wobble. Figure 2 shows that the observed excitation power (black curve) increases as the frequency approaches ±1/21 cpy, the lowest frequency that can be resolved with the 21-yearlong series studied here. However, the power of both the atmospheric excitation series and the sum of the atmospheric and oceanic excitation series remains relatively flat throughout the interannual and lower-frequency band of −1 cpy to +1 cpy, indicating that neither atmospheric nor oceanic processes have enough power to maintain the Markowitz wobble. However, like the pentadal wobbles, before atmospheric and oceanic processes can be eliminated as possible excitation mechanisms of the Markowitz wobble, series longer than the 21-yearlong series used here must be studied.

8. Intraseasonal Wobbles

[44] Like the seasonal and interannual wobbles, the wobbling motion of the Earth on intraseasonal timescales is a forced response of the Earth to its excitation mechanisms. *Eubanks et al.* [1988] studied the Earth's wobbles on timescales between 2 weeks and several months, concluding that these rapid polar motions during 1983.75–1986.75 are at least partially driven by atmospheric surface pressure changes. Subsequent studies [*Salstein and Rosen*, 1989; *Nastula et al.*, 1990; *Gross and Lindqwister*, 1992; *Nastula*, 1992, 1995, 1997; *Kuehne et al.*, 1993; *Salstein*, 1993; *Kosek et al.*, 1995; *Nastula and Salstein*, 1999; *Kolaczek et al.*, 2000a, 2000b] confirmed the importance of atmospheric processes in exciting rapid polar motions, although the

existence of significant discrepancies indicates that non-atmospheric processes may also play an important role.

[45] The contribution of oceanic processes to exciting rapid polar motions has been studied using both barotropic [*Ponte*, 1997; *Nastula and Ponte*, 1999] and baroclinic [*Ponte et al.*, 1998; *Johnson et al.*, 1999; *Nastula et al.*, 2000] models of the oceans. Such studies have shown that while better agreement with the observations is obtained when oceanic excitation is added to that of the atmosphere, significant discrepancies still remain. For example, using a barotropic ocean model, *Nastula and Ponte* [1999] obtained correlations of 0.80 and 0.88 between the *x* and *y* components, respectively, of the observed and sum of atmospheric and oceanic excitation functions for signals having periods between 15 and 150 days during 1993–1995. Despite these highly significant correlations, the observed variance in this intraseasonal frequency band was larger than the modeled atmospheric and oceanic variance, by about 10% for the *x* component, but by nearly a factor of 2 for the *y* component. Here, a baroclinic model of the oceans, the ECCO model, is used to study the contribution of oceanic processes to exciting intraseasonal wobbles during 1980–2000.

[46] Estimates of the coherence at high frequencies between the observed and sum of atmospheric and oceanic excitation functions used here (not shown) indicate a loss of coherence at periods shorter than about 5 days. A 5-day running mean was therefore applied to the excitation functions used here in order to eliminate signals having periods less than 5 days. A high-pass filter with a cutoff frequency of 1 cpy was then applied to the excitation functions in order to isolate the intraseasonal frequency band. As before, seasonal signals were first removed from the excitation functions by least squares fitting and removing a mean, a trend, and periodic terms at the annual, semiannual, and terannual frequencies. Thus the intraseasonal frequency band considered here consists of signals having periods between 5 days and 1 year excluding signals at the annual, semiannual, and terannual frequencies.

[47] Figure 8 shows the *x* and *y* components of the observed and modeled excitation functions on intraseasonal timescales during 1993. The atmospheric excitation function shown in Figure 8 (red curve) is the sum of wind and surface pressure excitation. Adding oceanic current and bottom pressure excitation to that of atmospheric winds and surface pressure (blue curve) is seen to improve the agreement with that observed (black curve). Results for other intervals during 1980–2000 are similar to that shown in Figure 8 for 1993.

[48] Table 6 gives the percentage of the observed excitation variance explained by the modeled excitation processes along with the correlation between the observed and modeled excitation series in the intraseasonal frequency band during 1980–2000. As in Table 5, *X* gives the results for the *x* component, *Y* gives the results for the *y* component, and *X + iY* gives the results for the complex-valued excitation functions formed from the *x* and *y* components. The 99% significance level for the correlations in the intraseasonal frequency band is estimated to be 0.08 after accounting for the reduction in the degrees of freedom that was determined from the width of the central peak of the autocorrelation functions.
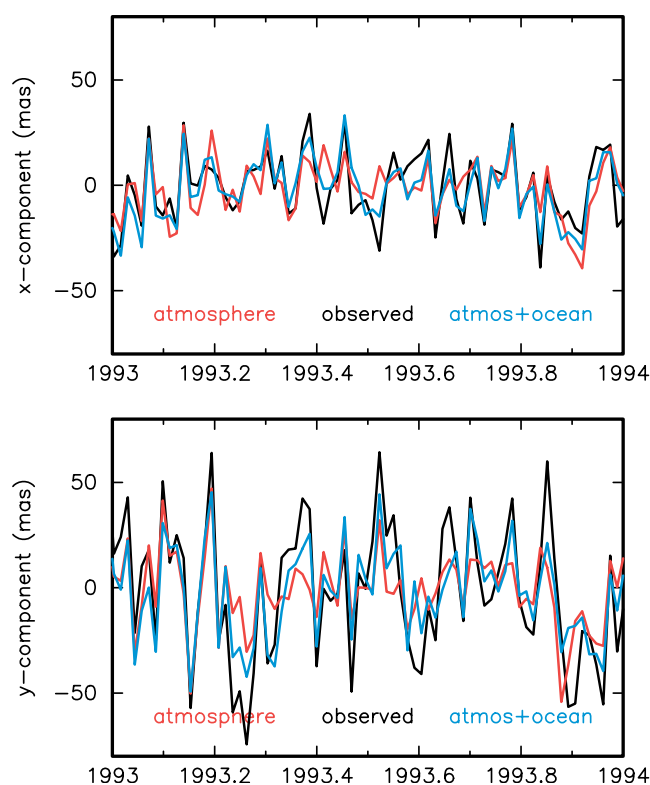
INTRASEASONAL EXCITATION

Figure 8. The x and y components of the observed (black), the sum of atmospheric wind and surface pressure (red), and the sum of atmospheric wind and surface pressure and oceanic currents and bottom pressure (blue) excitation functions on intraseasonal timescales during 1993. Intraseasonal wobbles are defined here to be wobbles having periods between 5 days and 1 year. The atmospheric surface pressure term is that computed assuming the ocean response to the imposed surface pressure variations is as an inverted barometer.

[49] As can be seen from Table 6, during 1980–2000 atmospheric processes are more effective in exciting intraseasonal wobbles than are oceanic processes. Atmospheric wind and surface pressure changes can explain 36.5% and 47.8%, respectively, of the x and y components of the observed intraseasonal wobble excitation, and have correlation coefficients with the observed x and y components of 0.61 and 0.69, respectively. Oceanic current and bottom pressure variations, however, can explain just 16.6% and 19.4%, respectively, of the observed x and y components and have correlation coefficients with them of 0.42 and 0.44, respectively. Thus oceanic processes are less than half as effective as atmospheric processes in exciting wobbles on intraseasonal timescales.

[50] Also seen from Table 6 is the importance of atmospheric surface and ocean bottom pressure changes in exciting intraseasonal wobbles. Surface and bottom pressure changes can explain 42.2% and 53.6%, respectively, of the x and y components of the observed intraseasonal wobble excitation, and have correlation coefficients with the observed x and y components of 0.65 and 0.76, respectively.

On the other hand, atmospheric winds and oceanic currents can explain just 20.9% and 28.6%, respectively, of the observed x and y components and have correlation coefficients with them of 0.46 and 0.61, respectively. Thus surface and bottom pressure changes are about twice as effective as winds and currents in exciting intraseasonal wobbles.

[51] During 1980–2000, the single most effective process in exciting intraseasonal wobbles is seen to be atmospheric surface pressure changes. Treating polar motion excitation as a complex-valued quantity, surface pressure changes explain about twice as much of the observed variance as do either wind or bottom pressure changes, and explain nearly 4 times as much of the observed variance as do oceanic currents. Overall, the sum of all complex-valued atmospheric and oceanic processes can explain 65.3% of the observed variance, they have a correlation coefficient of 0.81 with the observations, and their x and y components agree about equally well with the observations.

[52] About 1/3 of the observed excitation variance on intraseasonal timescales is not explained by the atmospheric and oceanic excitation functions used here. This discrepancy may be due to either uncertainties in the data sets used here, or to the effects of other excitation processes that have not been considered here. Table 6 gives results for the entire time interval studied here, namely, 1980–2000. During this time interval improvements to the polar motion observing systems have led to more accurate determinations of the observed polar motion excitation functions. For example, the median formal uncertainty of the daily COMB2000 polar motion excitation series during 1980 is 18 mas,

Table 6. Intraseasonal Wobble Excitation During 1980–2000[a]

Excitation Process	X	Y	$X + i Y$
Percent of Observation Excitation Variance Explained			
Atmospheric			
Wind	18.9	19.6	19.4
Surface pressure (IB)	21.3	38.2	33.5
Wind plus surface pressure (IB)	36.5	47.8	44.6
Oceanic			
Currents	3.1	10.4	8.4
Bottom pressure	17.8	14.6	15.5
Currents plus bottom pressure	16.6	19.4	18.6
Atmospheric plus oceanic			
Wind plus currents	20.9	28.6	26.5
Surface (IB) plus bottom pressure	42.2	53.6	50.4
Total of all atmospheric plus oceanic	61.3	66.9	65.3
Correlation of Observed Excitation			
Atmospheric			
Wind	0.44	0.52	0.49
Surface pressure (IB)	0.47	0.64	0.59
Wind plus surface pressure (IB)	0.61	0.69	0.67
Oceanic			
Currents	0.20	0.40	0.31
Bottom pressure	0.43	0.39	0.41
Currents plus bottom pressure	0.42	0.44	0.44
Atmospheric plus oceanic			
Wind plus currents	0.46	0.61	0.54
Surface (IB) plus bottom pressure	0.65	0.76	0.73
Total of all atmospheric plus oceanic	0.78	0.82	0.81

[a]X, x component; Y, y component; IB is inverted barometer; 99% significance level for correlations is 0.08; intraseasonal wobbles considered here have periods ranging between 5 days and 1 year excluding signals at the annual, semiannual, and terannual frequencies.

Table 7. Intraseasonal Wobble Excitation During 1993−2000[a]

Excitation Process	X	Y	$X + i\,Y$
Percent of Observation Excitation Variance Explained			
Atmospheric			
Wind	20.6	20.8	20.8
Surface pressure (IB)	20.0	39.5	34.3
Wind plus surface pressure (IB)	39.1	52.1	48.7
Oceanic			
Currents	4.6	11.1	9.4
Bottom pressure	22.9	17.7	19.1
Currents plus bottom pressure	23.3	23.6	23.5
Atmospheric plus oceanic			
Wind plus currents	23.5	30.1	28.4
Surface (IB) plus bottom pressure	45.1	56.8	53.7
Total of all atmospheric plus oceanic	68.7	72.3	71.4
Correlation of Observed Excitation			
Atmospheric			
Wind	0.47	0.56	0.52
Surface pressure (IB)	0.45	0.67	0.61
Wind plus surface pressure (IB)	0.63	0.74	0.71
Oceanic			
Currents	0.22	0.43	0.34
Bottom pressure	0.50	0.45	0.47
Currents plus bottom pressure	0.48	0.49	0.49
Atmospheric plus oceanic			
Wind plus currents	0.49	0.64	0.57
Surface (IB) plus bottom pressure	0.67	0.81	0.76
Total of all atmospheric plus oceanic	0.83	0.86	0.85

[a]X, x component; Y, y component; IB is inverted barometer; 99% significance level for correlations is 0.13; intraseasonal wobbles considered here have periods ranging between 5 days and 1 year excluding signals at the annual, semiannual, and terannual frequencies.

whereas during 2000 it is 8 mas. The atmospheric and oceanic excitation series used here can similarly be expected to have improved during 1980−2000.

[53] To test the impact of improvements in the observed and modeled excitation series used here, Table 7 gives the percentage of the observed excitation variance explained by the modeled excitation processes along with the correlation between the observed and modeled excitation functions during 1993−2000. As can be seen by comparing the entries in Table 7 with the respective entries in Table 6, better agreement between the observed and modeled excitation functions is obtained during this more recent time interval. Overall during 1993−2000, the sum of all complex-valued atmospheric and oceanic processes can explain 71.4% of the observed variance on intraseasonal timescales, and they have a correlation coefficient of 0.85 with the observations.

9. Discussion and Summary

[54] Atmospheric and oceanic excitation of the Earth's wobbles during 1980−2000 has been studied here using atmospheric angular momentum series estimated from the NCEP/NCAR reanalysis project and oceanic angular momentum series estimated from the ECCO consortium's simulation of the general circulation of the oceans. Atmospheric surface and ocean bottom pressure variations were found to be more effective than atmospheric wind and oceanic current changes in exciting the Earth's wobbles during this time interval. On intraseasonal and seasonal timescales, surface pressure changes were found to be the single most effective excitation mechanism, whereas on

interannual timescales the single most effective excitation mechanism was found to be ocean bottom pressure variations. Atmospheric wind and oceanic current changes were found to explain only 1/4 as much of the observed variance as atmospheric surface and ocean bottom pressure fluctuations on interannual timescales, and only 1/2 as much on intraseasonal timescales.

[55] While the sum of atmospheric wind and surface pressure and oceanic current and bottom pressure variations were shown to be coherent with and to have enough power to excite the Chandler wobble during 1980−2000, discrepancies exist between the observed and modeled excitation functions in the intraseasonal, seasonal, and interannual frequency bands. The discrepancy was smallest in the intraseasonal frequency band where atmospheric and oceanic processes can explain 61.3% and 66.9% of the observed variance in the x and y components, respectively, during 1980−2000, and 68.7% and 72.3% of it, respectively, during 1993−2000. However, the discrepancy was rather large in the interannual frequency band, particularly in the x component, where atmospheric and oceanic processes can explain only 7.5% and 50.8% of the observed variance in the x and y components, respectively, during 1980−2000.

[56] The discrepancy found between the observed and modeled excitation functions could be due to either errors in the excitation series, or to the action of other excitation processes that have not been considered here. Errors in the excitation functions are certainly a limiting factor in closing the excitation budget during 1980−2000. This is evident from the improved agreement between the observed and modeled excitation functions in the intraseasonal frequency band that is obtained when just the results during the more recent time interval of 1993−2000 is considered. Also, *Ponte et al.* [2001] have shown that better agreement with the observed excitation functions is obtained when using oceanic angular momentum series that have been estimated from an ocean model that has assimilated oceanographic data.

[57] However, the substantial discrepancy between the observed and modeled excitation functions in the interannual frequency band is unlikely to be solely due to errors in the excitation series. The large discrepancy in the interannual frequency band, particularly in the x component, indicates that other excitation processes that have not been considered here are needed to close the excitation budget, at least on these longer timescales. *Wünsch* [2002] has concluded that soil moisture and snow load effects are important contributors to exciting the annual and semiannual wobbles, and *Kuehne and Wilson* [1991] have concluded that the effects of terrestrial water storage may be an important excitation mechanism on interannual and longer timescales. The ability of water to be stored on land, either in the ground or on its surface as snow and ice, allows terrestrial water storage to be a potentially important mechanism in exciting the Earth's wobbles on seasonal and longer timescales.

[58] The redistribution of atmospheric, oceanic, and hydrologic mass, appearing as changes in atmospheric surface pressure, ocean bottom pressure, or terrestrial water storage, are important mechanisms in exciting the Earth's wobbles. Such redistribution of mass also causes the Earth's gravitational field to change, an effect which is currently being

measured by the CHAMP satellite mission and which will soon be measured by the GRACE satellite mission. Thus CHAMP and GRACE will, in effect, be directly measuring the excitation of the Earth's wobbles caused by mass redistribution. The availability of direct measurements of the excitation due to mass redistribution over land and, separately, within the oceans can be expected to lead to greater understanding of the mechanisms exciting the Earth's wobbles.

References

Abarca del Rio, R., and A. Cazenave, Interannual variations in the Earth's polar motion for 1963–1991: Comparison with atmospheric angular momentum over 1980–1991, *Geophys. Res. Lett.*, *21*, 2361–2364, 1994.

Aoyama, Y., and I. Naito, Atmospheric excitation of the Chandler wobble, 1983–1998, *J. Geophys. Res.*, *106*, 8941–8954, 2001.

Barnes, R. T. H., R. Hide, A. A. White, and C. A. Wilson, Atmospheric angular momentum fluctuations, length-of-day changes and polar motion, *Proc. R. Soc. London, Ser. A*, *387*, 31–73, 1983.

Barnier, B., L. Siefridt, and P. Marchesiello, Thermal forcing for a global ocean circulation model using a three-year climatology of ECMWF analyses, *J. Mar. Syst.*, *6*, 363–380, 1995.

Brzezinski, A., Polar motion excitation by variations of the effective angular momentum function: Considerations concerning deconvolution problem, *Manuscr. Geod.*, *17*, 3–20, 1992.

Brzezinski, A., and J. Nastula, Oceanic excitation of the Chandler wobble, *Adv. Space Res.*, *30*, 195–200, 2002.

Brzezinski, A., J. Nastula, and R. M. Ponte, Oceanic excitation of the Chandler wobble using a 50-year time series of ocean angular momentum, in *Vistas for Geodesy in the New Millennium, IAG Symp.*, vol. 125, edited by J. Adám and K.-P. Schwarz, pp. 434–439, Springer-Verlag, New York, 2002.

Chao, B. F., Excitation of the Earth's polar motion due to mass variations in major hydrological reservoirs, *J. Geophys. Res.*, *93*, 13,811–13,819, 1988.

Chao, B. F., and A. Y. Au, Atmospheric excitation of the Earth's annual wobble: 1980–1988, *J. Geophys. Res.*, *96*, 6577–6582, 1991.

Chao, B. F., and R. S. Gross, Changes in the Earth's rotation and low-degree gravitational field introduced by earthquakes, *Geophys. J. R. Astron. Soc.*, *91*, 569–596, 1987.

Chao, B. F., and W. P. O'Connor, Effect of a uniform sea-level change on the Earth's rotation and gravitational field, *Geophys. J. R. Astron. Soc.*, *93*, 191–193, 1988.

Chao, B. F., and Y.-H. Zhou, Meteorological excitation of interannual polar motion by the North Atlantic Oscillation, *J. Geodyn.*, *27*, 61–73, 1999.

Chao, B. F., W. P. O'Connor, A. T. C. Chang, D. K. Hall, and J. L. Foster, Snow load effect on the Earth's rotation and gravitational field, 1979–1985, *J. Geophys. Res.*, *92*, 9415–9422, 1987.

Chao, B. F., R. D. Ray, J. M. Gipson, G. D. Egbert, and C. Ma, Diurnal/semidiurnal polar motion excited by oceanic tidal angular momentum, *J. Geophys. Res.*, *101*, 20,151–20,163, 1996.

Chen, J. L., C. R. Wilson, R. J. Eanes, and B. D. Tapley, A new assessment of long-wavelength gravitational variations, *J. Geophys. Res.*, *105*, 16,271–16,277, 2000a.

Chen, J. L., C. R. Wilson, B. F. Chao, C. K. Shum, and B. D. Tapley, Hydrological and oceanic excitations to polar motion and length-of-day variation, *Geophys. J. Int.*, *141*, 149–156, 2000b.

Eubanks, T. M., Variations in the orientation of the Earth, in *Contributions of Space Geodesy to Geodynamics: Earth Dynamics, Geodyn. Ser.*, vol. 24, edited by D. E. Smith and D. L. Turcotte, pp. 1–54, AGU, Washington, D. C., 1993.

Eubanks, T. M., J. A. Steppe, J. O. Dickey, R. D. Rosen, and D. A. Salstein, Causes of rapid motions of the Earth's pole, *Nature*, *334*, 115–119, 1988.

Gipson, J. M., Very long baseline interferometry determination of neglected tidal terms in high-frequency Earth orientation variation, *J. Geophys. Res.*, *101*, 28,051–28,064, 1996.

Greatbatch, R. J., A note on the representation of steric sea level in models that conserve volume rather than mass, *J. Geophys. Res.*, *99*, 12,767–12,771, 1994.

Greatbatch, R. J., Y. Lu, and Y. Cai, Relaxing the Boussinesq approximation in ocean circulation models, *J. Atmos. Oceanic Technol.*, *18*, 1911–1923, 2001.

Gross, R. S., Correspondence between theory and observations of polar motion, *Geophys. J. Int.*, *109*, 162–170, 1992.

Gross, R. S., The effect of ocean tides on the Earth's rotation as predicted by the results of an ocean tide model, *Geophys. Res. Lett.*, *20*, 293–296, 1993.

Gross, R. S., The excitation of the Chandler wobble, *Geophys. Res. Lett.*, *27*, 2329–2332, 2000.

Gross, R. S., Combinations of Earth orientation measurements: SPACE2000, COMB2000, and POLE2000, *JPL Publ., 01-2*, 25 pp., 2001a.

Gross, R. S., Gravity, oceanic angular momentum, and the Earth's rotation, in *Gravity, Geoid, and Geodynamics 2000, IAG Symp.*, vol. 123, edited by M. G. Sideris, pp. 153–158, Springer-Verlag, New York, 2001b.

Gross, R. S., CHAMP, mass displacements, and the Earth's rotation, in *First CHAMP Mission Results for Gravity, Magnetic, and Atmospheric Studies*, edited by C. Reigber, H. Lühr, and P. Schwintzer, pp. 174–179, Springer-Verlag, New York, 2003.

Gross, R. S., and U. J. Lindqwister, Atmospheric excitation of polar motion during the GIG '91 measurement campaign, *Geophys. Res. Lett.*, *19*, 849–852, 1992.

Gross, R. S., K. H. Hamdan, and D. H. Boggs, Evidence for excitation of polar motion by fortnightly ocean tides, *Geophys. Res. Lett.*, *23*, 1809–1812, 1996.

Gross, R. S., B. F. Chao, and S. Desai, Effect of long-period ocean tides on the Earth's polar motion, *Prog. Oceanogr.*, *40*, 385–397, 1997.

Gross, R. S., T. M. Eubanks, J. A. Steppe, A. P. Freedman, J. O. Dickey, and T. F. Runge, A Kalman filter-based approach to combining independent Earth orientation series, *J. Geod.*, *72*, 215–235, 1998.

Herring, T. A., and D. Dong, Measurement of diurnal and semidiurnal rotational variations and tidal parameters of Earth, *J. Geophys. Res.*, *99*, 18,051–18,071, 1994.

Johnson, T. J., C. R. Wilson, and B. F. Chao, Oceanic angular momentum variability estimated from the Parallel Ocean Climate Model, 1988–1998, *J. Geophys. Res.*, *104*, 25,183–25,195, 1999.

Kalnay, E., et al., The NCEP/NCAR 40-year reanalysis project, *Bull. Am. Meteorol. Soc.*, *77*, 437–471, 1996.

Kolaczek, B., W. Kosek, and H. Schuh, Short-period oscillations of Earth rotation, in *Polar Motion: Historical and Scientific Problems, IAU Colloq.*, vol. 178, edited by S. Dick, D. McCarthy, and B. Luzum, pp. 533–544, Astron. Soc. of the Pac., San Francisco, Calif., 2000a.

Kolaczek, B., M. Nuzhdina, J. Nastula, and W. Kosek, El Niño impact on atmospheric polar motion excitation, *J. Geophys. Res.*, *105*, 3081–3087, 2000b.

Kosek, W., J. Nastula, and B. Kolaczek, Variability of polar motion oscillations with periods from 20 to 150 days in 1979–1991, *Bull. Geod.*, *69*, 308–319, 1995.

Kuehne, J., and C. R. Wilson, Terrestrial water storage and polar motion, *J. Geophys. Res.*, *96*, 4337–4345, 1991.

Kuehne, J., S. Johnson, and C. R. Wilson, Atmospheric excitation of nonseasonal polar motion, *J. Geophys. Res.*, *98*, 19,973–19,978, 1993.

Levitus, S., and T. P. Boyer, *World Ocean Atlas 1994*, vol. 4, *Temperature, NOAA Atlas NESDIS*, vol. 4, 129 pp., Natl. Oceanic and Atmos. Admin., Silver Spring, Md., 1994.

Levitus, S., R. Burgett, and T. P. Boyer, *World Ocean Atlas 1994*, vol. 3, *Salinity, NOAA Atlas NESDIS*, vol. 3, 111 pp., Natl. Oceanic and Atmos. Admin., Silver Spring, Md., 1994.

Marshall, J., C. Hill, L. Perelman, and A. Adcroft, Hydrostatic, quasi-hydrostatic, and nonhydrostatic ocean modeling, *J. Geophys. Res.*, *102*, 5733–5752, 1997a.

Marshall, J., A. Adcroft, C. Hill, L. Perelman, and C. Heisey, A finite-volume, incompressible, Navier Stokes model for studies of the ocean on parallel computers, *J. Geophys. Res.*, *102*, 5753–5766, 1997b.

Mathews, P. M., T. A. Herring, and B. A. Buffett, Modeling of nutation and precession: New nutation series for nonrigid Earth and insights into the Earth's interior, *J. Geophys. Res.*, *107*(B4), 2068, doi:10.1029/2001JB000390, 2002.

McCarthy, D. D., (Ed.), IERS conventions (1996), *IERS Tech. Note 21*, 97 pp., Obs. de Paris, Paris, 1996.

Munk, W. H., and G. J. F. MacDonald, *The Rotation of the Earth: A Geophysical Discussion*, 323 pp., Cambridge Univ. Press, New York, 1960.

Nastula, J., Short periodic variations in the Earth's rotation in the period 1984–1990, *Ann. Geophys.*, *10*, 441–448, 1992.

Nastula, J., Short periodic variations of polar motion and hemispheric atmospheric angular momentum excitation functions in the period 1984–1992, *Ann. Geophys.*, *13*, 217–225, 1995.

Nastula, J., The regional atmospheric contributions to the polar motion and EAAM excitation functions, in *Gravity, Geoid, and Marine Geodesy, IAG Symp.*, vol. 117, edited by J. Segawa, H. Fujimoto, and S. Okubo, pp. 281–288, Springer-Verlag, New York, 1997.

Nastula, J., and R. M. Ponte, Further evidence for oceanic excitation of polar motion, *Geophys. J. Int.*, *139*, 123–130, 1999.

Nastula, J., and D. Salstein, Regional atmospheric angular momentum contributions to polar motion excitation, *J. Geophys. Res.*, *104*, 7347–7358, 1999.

Nastula, J., D. Gambis, and M. Feissel, Correlated high-frequency variations in polar motion and length of the day in early 1988, *Ann. Geophys.*, *8*, 565–570, 1990.

Nastula, J., R. M. Ponte, and D. A. Salstein, Regional signals in atmospheric and oceanic excitation of polar motion, in *Polar Motion: Historical and Scientific Problems*, *IAU Colloq.*, vol. 178, edited by S. Dick, D. McCarthy, and B. Luzum, pp. 463–472, Astron. Soc. of the Pac., San Francisco, Calif., 2000.

Percival, D. B., and A. T. Walden, *Spectral Analysis for Physical Applications: Multitaper and Conventional Univariate Techniques*, 610 pp., Cambridge Univ. Press, New York, 1993.

Ponte, R. M., Oceanic excitation of daily to seasonal signals in Earth rotation: Results from a constant-density numerical model, *Geophys. J. Int.*, *130*, 469–474, 1997.

Ponte, R. M., and D. Stammer, Role of ocean currents and bottom pressure variability on seasonal polar motion, *J. Geophys. Res.*, *104*, 23,393–23,409, 1999.

Ponte, R. M., D. Stammer, and J. Marshall, Oceanic signals in observed motions of the Earth's pole of rotation, *Nature*, *391*, 476–479, 1998.

Ponte, R. M., D. Stammer, and C. Wunsch, Improving ocean angular momentum estimates using a model constrained by data, *Geophys. Res. Lett.*, *28*, 1775–1778, 2001.

Priestley, M. B., *Spectral Analysis and Time Series*, 957 pp., Academic, San Diego, Calif., 1981.

Reynolds, R. W., and T. M. Smith, Improved global sea surface temperature analyses using optimum interpolation, *J. Clim.*, *7*, 929–948, 1994.

Salstein, D. A., Monitoring atmospheric winds and pressures for Earth orientation studies, *Adv. Space Res.*, *13*(11), 175–184, 1993.

Salstein, D. A., and R. D. Rosen, Regional contributions to the atmospheric excitation of rapid polar motions, *J. Geophys. Res.*, *94*, 9971–9978, 1989.

Salstein, D. A., and R. D. Rosen, Global momentum and energy signals from reanalysis systems, paper presented at Seventh Conference on Climate Variations, Am. Meteorol. Soc., Boston, Mass., 1997.

Salstein, D. A., D. M. Kann, A. J. Miller, and R. D. Rosen, The Sub-bureau for Atmospheric Angular Momentum of the International Earth Rotation Service: A meteorological data center with geodetic applications, *Bull. Am. Meteorol. Soc.*, *74*, 67–80, 1993.

Sovers, O. J., C. S. Jacobs, and R. S. Gross, Measuring rapid ocean tidal Earth orientation variations with VLBI, *J. Geophys. Res.*, *98*, 19,959–19,971, 1993.

Trupin, A. S., Effects of polar ice on the Earth's rotation and gravitational potential, *Geophys. J. Int.*, *113*, 273–283, 1993.

Trupin, A. S., M. F. Meier, and J. M. Wahr, Effect of melting glaciers on the Earth's rotation and gravitational field: 1965–1984, *Geophys. J. Int.*, *108*, 1–15, 1992.

Wahr, J. M., The effects of the atmosphere and oceans on the Earth's wobble - I. Theory, *Geophys. J. R. Astron. Soc.*, *70*, 349–372, 1982.

Wahr, J. M., The effects of the atmosphere and oceans on the Earth's wobble and on the seasonal variations in the length of day - II. Results, *Geophys. J. R. Astron. Soc.*, *74*, 451–487, 1983.

Wilson, C. R., Contributions of water mass redistribution to polar motion excitation, in *Contributions of Space Geodesy to Geodynamics: Earth Dynamics*, *Geodyn. Ser.*, vol. 24, edited by D. E. Smith and D. L. Turcotte, pp. 77–82, AGU, Washington, D. C., 1993.

Wilson, C. R., and R. O. Vicente, Maximum likelihood estimates of polar motion parameters, in *Variations in Earth Rotation*, *Geophys. Monogr. Ser.*, vol. 59, edited by D. D. McCarthy and W. E. Carter, pp. 151–155, AGU, Washington, D. C., 1990.

Wünsch, J., Oceanic and soil moisture contributions to seasonal polar motion, *J. Geodyn.*, *33*, 269–280, 2002.

———————————

I. Fukumori, R. S. Gross, and D. Menemenlis, Jet Propulsion Laboratory, California Institute of Technology, 4800 Oak Grove Drive, Pasadena, CA 91109-8099, USA. (richard.gross@jpl.nasa.gov)